

A MODEL FOR THE MOVING ‘WISPS’ IN THE CRAB NEBULA

MITCHELL C. BEGELMAN¹JILA, University of Colorado and National Institute of Standards and Technology
Campus Box 440, Boulder, CO 80309-0440; mitch@jila.colorado.edu*To Appear in The Astrophysical Journal; Feb. 20, 1999; Volume 512*

ABSTRACT

I propose that the moving ‘wisps’ near the center of the Crab Nebula result from nonlinear Kelvin-Helmholtz instabilities in the equatorial plane of the shocked pulsar wind. Recent observations suggest that the wisps trace out circular wavefronts in this plane, expanding radially at speeds $\lesssim c/3$. Instabilities could develop if there is sufficient velocity shear between a faster-moving equatorial zone and a slower moving shocked pulsar wind at higher latitudes. The development of shear could be related to the existence of a neutral sheet — with weak magnetic field — in the equatorial zone, and could also be related to a recent suggestion by Begelman that the magnetic field in the Crab pulsar wind is much stronger than had been thought. I show that plausible conditions could lead to the growth of instabilities at the radii and speeds observed, and that their nonlinear development could lead to the appearance of sharp wisplike features.

Subject headings: radiation mechanisms: instabilities — ISM: individual (Crab Nebula) — ISM: jets and outflows — pulsars: individual: Crab pulsar — supernova remnants

1. INTRODUCTION

Recent observations have clarified the geometry and kinematics of the bright optical arcs, commonly known as ‘wisps,’ that are situated $\approx 7 - 15''$ northwest of the Crab pulsar. The variability of these features has been known for decades (Lampland 1921; Oort & Walraven 1956; Scargle 1969), but as recently as 1995 it was still unclear whether they fluctuated in position and/or intensity, or exhibited coherent motion (Hester et al. 1995). Systematic monitoring over a period of 3.5 years by Tanvir, Thomson, & Tsikarishvili (1997) now seems to establish that the wisps move radially outward from the pulsar, with speeds $\lesssim c/3$ (assuming a distance to the Crab of 2 kpc). Moreover, the wisps appear to represent approaching segments of circular wavefronts confined to the equatorial plane of the pulsar, which is tipped $\sim 30^\circ$ to the line of sight. High resolution images of the wisps (Hester et al. 1995), obtained with the WFPC2 on board *Hubble Space Telescope* show that the wisps are extremely narrow ($\sim 0.2''$ in width), with synchrotron surface brightnesses exceeding the immediate background by an order of magnitude or more.

A few models in the literature have attempted to explain the physical nature of the wisps. A large fraction of the Crab pulsar’s spindown energy is thought to emerge via a relativistic, magnetohydrodynamic wind, which suffers a strong shock in the vicinity of the wisps (Rees & Gunn 1974; Kennel & Coroniti 1984). The detailed model by Gallant & Arons (1994) associates the multiple wisps with internal structure in the pulsar wind termination shock. Other models interpret the wisps as propagating magnetosonic (Woltjer 1958; Barnes & Scargle 1973) or drift (Chedia et al. 1997) waves. Lou (1996, 1998) regards the wisps as originating in the ultrarelativistic wind upstream of the shock. Hester et al. (1995) propose that the wisps are instabilities driven by synchrotron cooling in the flow.

Other modelers have regarded the wisps as generically associated with the wind termination shock, at various levels of detail (e.g., Rees & Gunn 1974; Kundt & Krotscheck 1980; Kennel & Coroniti 1984). These models have varying degrees of success in explaining the systematic outward motion found by Tanvir et al. (1997).

In this paper I present a new model that can account for the wisps’ systematic outward velocity, their apparent confinement to a thin equatorial sheet in the pulsar wind, and their sharp brightness profiles. I propose that a narrow equatorial zone of the shocked pulsar wind is moving somewhat faster than the wind at higher latitudes. The thin equatorial zone can be identified physically with the ‘neutral sheet’ across which the direction of the toroidal magnetic field reverses. Such a zone must be present in any pulsar wind. In § 4 I will discuss physical effects that may give rise to the shear, but for the present I will simply assume that it exists. The shear between the zones gives rise to Kelvin-Helmholtz (K-H) instabilities which cause the equatorial sheet to ripple. If the sheet is radiating and the ripples grow to sufficiently nonlinear amplitudes, then the surface brightness distribution of the sheet will exhibit narrow, bright arcs that can be identified as the wisps. In § 2 I discuss the K-H instability as it may apply in the shocked pulsar wind, and show that it can lead to ripples with roughly the observed spacings and pattern speeds. In § 3 I show how our line of sight through a sufficiently rippled, emitting sheet can give rise to sharp arc-like features on the near and far sides of the sheet (with the leading side favored due to the Doppler effect), regardless of whether additional dissipative effects operate in the sheet. Finally, in § 4 I discuss possible reasons for the development of shear and observational implications of the model.

¹Also Department of Astrophysical and Planetary Sciences, University of Colorado, Boulder

2. KELVIN-HELMHOLTZ INSTABILITY OF THE SHEAR ZONE

For the purpose of a stability analysis, we model the equilibrium state of the equatorial shear zone as a uniform plane-parallel slab of unmagnetized relativistic fluid, with thickness $2H$ in the z -direction, moving with velocity $uc\hat{x}$ with respect to a stationary background medium. The exterior fluid also has a relativistic equation of state, as well as containing a uniform magnetic field oriented perpendicular to the flow velocity, $B_{\text{ex}}\hat{y}$. The assumption of a negligible magnetic field in the equatorial zone is motivated by its identification with the neutral sheet in the pulsar wind. We parameterize the field strength in the high-latitude region by its beta-parameter with respect to the external gas pressure, $\beta \equiv 8\pi P_{\text{ex}}/B_{\text{ex}}^2$. Pressure balance in the z -direction then requires the pressure in the unmagnetized slab to satisfy $P_{\text{in}} = P_{\text{ex}} + B_{\text{ex}}^2/8\pi$. Note that the particle densities in both fluids are irrelevant since the inertia is dominated by the relativistic energy density.

The Kelvin-Helmholtz (K-H) instability for a slab geometry with various physical conditions has been discussed extensively in the literature (e.g., Gill 1965; Ferrari, Massaglia, & Trussoni 1982; Payne & Cohn 1985; Hardee & Norman 1988; Hardee et al. 1992). Since the plane-parallel model is intended to approximate axisymmetric radial flow, we consider only modes propagating parallel to the flow velocity. Given perturbations of the form $f(z)\exp[i(\omega t - kx)]$, it is straightforward to derive the dispersion relation for the specified conditions. Defining the dimensionless quantities $w \equiv \omega H/c$, $\nu \equiv kc/\omega$, and

$$\kappa_1^2 = \frac{3(1-\nu u)^2 - (\nu - u)^2}{1-u^2}, \quad (1)$$

$$\kappa_2^2 = \nu^2 - \frac{3(1+2\beta)}{(3+2\beta)}, \quad (2)$$

$$\mathcal{A} = \frac{(1-u^2)(2\beta+1)}{2(\beta+1)(1-\nu u)^2\kappa_2}, \quad (3)$$

we obtain

$$\tan(w\kappa_1) = -\mathcal{A}\kappa_1 \quad (4)$$

for the modes that are antisymmetric (AS) about $z = 0$ (kink modes), and $\cot(w\kappa_1) = \mathcal{A}\kappa_1$ for the symmetric (S, or pinch) modes. The form of the dispersion relation given above is analogous to that introduced by Gill (1965) and used by many subsequent authors. For example, to relate our variables to the nonrelativistic magnetohydrodynamic limit studied by Hardee et al. (1992), we make the following identifications with their parameters β_{in} , β_{ex} , χ_{in} , χ_{ex} : $\kappa_1 \rightarrow \beta_{\text{in}}H/w$, $\kappa_2 \rightarrow i\beta_{\text{ex}}H/w$, $\mathcal{A} \rightarrow -(\chi_{\text{ex}}H)/(\chi_{\text{in}}w\kappa_2)$. To satisfy boundary conditions at $|z| \rightarrow \infty$, the real part of $w\kappa_2$ must be positive. Note that special relativistic effects are included in the derivation.

The mode structure predicted by eqs. (1)–(4) is qualitatively similar to that found in nonrelativistic treatments of slab jets, both with and without magnetic fields (Hardee & Norman 1988; Hardee et al. 1992). We are interested in the spatial growth of modes with real driving frequencies, so we set ω (and w) real and $k = k_R + ik_I$; $k_I > 0$ then corresponds to a growing mode. In addition to the fundamental AS and S modes which are unstable at all flow velocities, internal reflection modes appear when the

flow is sufficiently supersonic (and supermagnetosonic; see Hardee et al. 1992). However, these latter modes have phase and group velocities that exceed the effective sound speeds in both the unmagnetized ($c/\sqrt{3}$) and magnetized ($> c/\sqrt{3}$) regions. If Tanvir et al. (1997) are correct that the wisps move outward at speeds $\lesssim c/3$, then the pattern speed is highly *subsonic*.

We will assume (based on the appearance of the wisps; see § 3) that we are dealing with the fundamental AS mode in the long-wavelength limit, $|kH| \ll 1$. We can then approximate the dispersion relation by $\mathcal{A} + w \approx 0$. These modes correspond to side-to-side displacements — ripples — of the slab. Since the e -folding length of the instability, k_I^{-1} , is a monotonically decreasing function of ω , all wavelengths shorter than a certain value will have reached nonlinearity at any given radius in the wind. We will associate the wisps with the *longest* wavelength (i.e., lowest frequency) modes that have room to grow, since these are expected to dominate the large-scale structure of the ripples. Thus, the dominant modes have $k_I \sim \text{few} \times r^{-1}$, where r is the radius at which the ripples appear.

Phase velocities $v_p = \omega/k_{RC} \equiv \nu_R^{-1}$ of very-long-wavelength modes vary as $v_p \propto (kH)^{1/2} \propto \omega^{1/3}$, i.e., they decrease with increasing wavelength and decreasing frequency. The observed pattern speed of a weakly unstable linear wave packet is the group velocity, $\partial\omega/\partial k_R$, but the physical significance of this quantity is ill-defined for modes with $k_I \sim k_R$, as is the case here. Moreover, we are considering modes that have grown to nonlinear amplitudes, by which point the pattern speeds may have changed. In their numerical simulations of nonrelativistic slab jets, Norman & Hardee (1988) find that the linear phase velocity gives a more accurate estimate of the nonlinear pattern speed than does the group velocity, and we will adopt this assumption here. Therefore, if the high-latitude wind has decelerated to $\ll c/3$ at the point at which we see the wisps, then the equatorial wind would have to be traveling with speed uc significantly faster than $c/3$ (from a relativistic point of view) in order to obtain the observed pattern speeds of $\sim c/3$. Note that the standard spherical shocked wind model for the Crab Nebula (Rees & Gunn 1974) predicts decreasing subsonic velocities $\sim (c/3)(r/r_s)^{-2}$ outside the shock radius, r_s . (The exact radial dependence is sensitive to the two-dimensional flow pattern.) Even if the equatorial wind speed significantly exceeded $c/3$, it would not necessarily have to be highly supersonic (i.e., $> c/\sqrt{3} \sim 0.58c$). Figure 1 shows $k_R H$ (solid lines) and $k_I H$ (dashed lines) as a function of slab velocity u , for negligible ($\beta \rightarrow \infty$: heavy lines) and equipartition ($\beta = 1$: light lines) magnetic fields, with the phase velocity fixed at $1/3$. The magnetic field strength has little effect on the curves. Note also that kH is already quite small ($\lesssim 0.15$) for transonic flow ($u = 0.58$), and decreases steadily for higher flow velocities.

Setting $\nu_R^{-1} = 1/3$ corresponds to the case in which the outflow speed of the high-latitude wind can be neglected. If the high-latitude wind were still moving outward at a sizable fraction of $c/3$ in the wisp region, then similar net pattern speeds could be attained with a slower equatorial wind. In this case, it would be even easier to obtain very small values of $|kH|$, which are desirable for producing sharp, intense wisp features (see § 3). Note, however,

that the limiting case of an equatorial wind moving only slightly faster than the high-latitude wind is not conducive to producing wisps with the observed spacing through K-H instability, since the modes would be advected outward before they had time to grow.

At the end of the epoch studied by Tanvir et al. (1997), there were two bright wisps roughly $7''$ and $15''$ from the pulsar. If we argue that the wavelength $2\pi/k_R$ of the dominant wisp mode is approximately $r/2$ and that this corresponds to ~ 6 growth lengths (consistent with fact that $k_I \sim k_R$), then we have $k_R r \sim 4\pi$. From the above estimates based on the theory of K-H instability, we expect $k_R H \lesssim 0.1$ for $u \gtrsim 0.6$, implying that the modes potentially have aspect ratios $r/8H \gtrsim 16$. The ratio can be much larger if the equatorial wind is faster than $0.6c$ or if the speed of the high-latitude wind is taken into account. These values are in the range required to obtain the observed narrowness and brightness contrasts of the wisps from viewing angle effects, as we shall now describe.

3. NARROW, BRIGHT FEATURES FROM A RIPPLED SHEET

Two of the most striking features of the wisps are their narrowness and their brightness contrast with respect to the local background. Assuming that the wisps are cylindrical filaments, Hester et al. (1995) estimated their equipartition (i.e., minimum) pressures at 28–54 times the mean equipartition pressure in the nebula ($\langle P_{\text{eq}} \rangle \sim 7 \times 10^{-9}$ dyne cm $^{-2}$; Trimble 1982). If the wisps were highly overpressured with respect to the *local* medium, then they would have to be out of dynamical equilibrium with their surroundings, i.e., they would have to be shocks. In our observing frame these putative strong shocks are traveling *downstream* at $\sim c/3$, but in the fluid frame they would have to be traveling *upstream* at somewhat more than the sound speed, $c/\sqrt{3}$. Applying the relativistic velocity addition law, this would imply that the equatorial wind would have to be traveling outward at highly supersonic speed, $\gtrsim 0.8c$. This is difficult to reconcile with the hypothesis that the wisps exist in the postshock region where the wind is subsonic or, at best, mildly supersonic.

Even if the equatorial wind is highly supersonic in the wisp region, it is hard to imagine what would create a set of shocks that always move outward at $\sim c/3$. Suppose the high-latitude wind went through a shock at r_s , but the equatorial wind punched through and remained supersonic. The sudden jump in pressure would drive oblique shocks into the equatorial wind as it crossed r_s , with the obliquity adjusted so that the shock fronts track the position of r_s . Thus, these shocks would not move systematically outward unless r_s also moved systematically outward, which seems unlikely. Similarly, internal shocks caused by intrinsic fluctuations in the wind should exhibit both inward and outward motions.

Fortunately, the high surface brightnesses can be explained without resorting to large overpressures. First, the mean pressure in the Crab may well be several times larger than the equipartition pressure. Moreover, the local pressure in the center of the nebula may be several times the nebular mean, due to magnetic tension effects (Kennel & Coroniti 1984; Begelman & Li 1992). A simple theory of the wind termination shock gives the pressure just downstream from the shock as $P_s \sim 9 \times 10^{-9} (L_w/5 \times 10^{38} \text{ erg s}^{-1}) (r_s/0.1 \text{ pc})^{-2}$ dyne cm $^{-2}$, where L_w is the

wind power. Recall that we are associating the wisps with K-H modes that grow downstream from the shock. Since the inner wisp is situated at ~ 0.1 pc, the actual radius of the shock might be 2–3 times smaller, suggesting that the ambient pressure in the wisp region could be as much as ~ 4 –10 times larger than $\langle P_{\text{eq}} \rangle$. Second, Doppler boosting will cause one to overestimate the equipartition pressure in the approaching wisps by a factor $\sim \mathcal{D}^{1.5}$, where \mathcal{D} is the Doppler factor (Heinz & Begelman 1997). For wind speeds $\gtrsim 0.5c$ and viewing angles $\approx 30^\circ$, this leads to a further decrease in the intrinsic equipartition pressure by a factor ~ 2 .

The remaining factor ~ 3 –6 in inferred overpressure can be explained away if we interpret the wisps not as cylindrical filaments but as thin radiating sheets, viewed nearly edge-on. This geometry can arise naturally from the nonlinear development of antisymmetric Kelvin-Helmholtz modes in a thin equatorial wind, provided that $k_R H$ is sufficiently small and the amplitude of the ripples grows sufficiently large. If the equatorial wind has uniform emissivity and the depth of our line of sight through the wind is $2\eta H \gg H$, then the inferred equipartition pressure goes down by a factor $\sim \eta^{-1/2}$. Thus, a depth-to-width ratio of $\eta \sim 10$ –30 is probably sufficient to explain the observed surface brightness in the wisps. These ratios are consistent with the predictions of the Kelvin-Helmholtz instability, provided that the viewing geometry is favorable.

This simple model can account not only for the brightness enhancement in the wisps, but also for their narrowness and their apparent confinement to a pair of arcs along the near and far sides of the wavefront. To illustrate this, we consider a rippled axisymmetric slab with upper and lower surfaces (at some fixed time) given by

$$z'_\pm = H(\pm 1 + a \sin kr') \quad (5)$$

where $r' = (x'^2 + y'^2)^{1/2}$ in terms of Cartesian coordinates defined in the equatorial plane of the slab. Now suppose we observe the slab along a line of sight in the $x' - z'$ plane, at an angle $\theta \approx 30^\circ$ from the slab's equator. We define observer's coordinates (x, y, z) according to $x' = x \csc \theta - z \cos \theta$, $y' = y$, $z' = z \sin \theta$, where (x, y) lie in the sky-plane and z denotes position along the line of sight. Our line of sight enters and exits the slab at

$$z_\pm = H \csc \theta \left[\pm 1 + a \sin \left(kr_0 - \frac{kx \cot \theta}{r_0} z_\pm \right) \right], \quad (6)$$

where $r_0 = (x^2 \csc^2 \theta + y^2)^{1/2}$ and we have neglected terms of second- and higher order in z_\pm/r_0 .

If the slab radiates uniformly, its brightness is proportional to the length of the line of sight between the entrance and exit points, $(z_+ - z_-)$. Since the unrippled slab ($a = 0$) has uniform brightness $2H \csc \theta$, we can quantify the enhancement due to rippling through the multiplicative factor

$$\Delta \equiv (z_+ - z_-) \sin \theta / 2H. \quad (7)$$

Defining the quantities $s \equiv (z_+ + z_-) \sin \theta / 2H$ and $q \equiv khx \cos \theta / (r_0 \sin^2 \theta)$, we can determine Δ from the following pair of equations:

$$\Delta = 1 - a \sin(q\Delta) \cos(kr_0 - qs) \quad (8)$$

$$s = a \cos(q\Delta) \sin(kr_0 - qs). \quad (9)$$

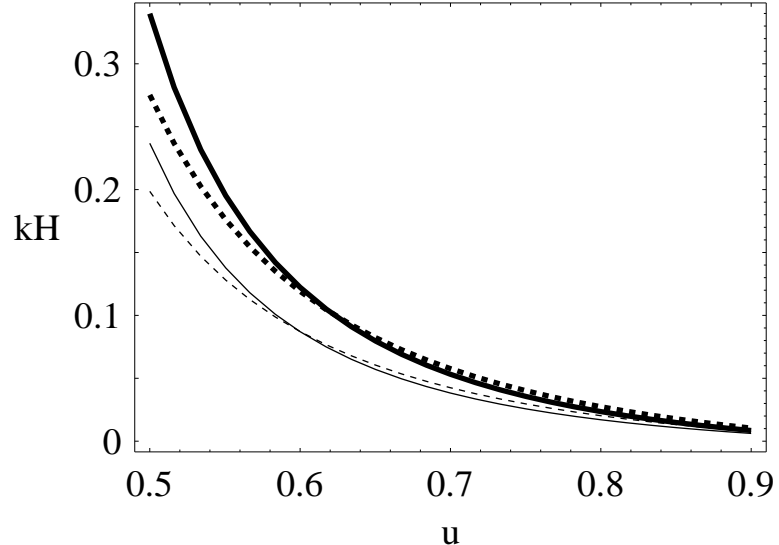


FIG. 1.— Real (solid) and imaginary (dashed) parts of kH as a function of the slab speed uc , assuming a phase velocity ω/k_R fixed at $c/3$. Heavy and light curves correspond to negligible and equipartition values of the ambient magnetic field, respectively.

For fixed a and q (corresponding to a fixed position angle on the sky, relative to the center of the slab), maximum values of Δ occur for $s = 0$ and $\sin kr_0 = 0$, and satisfy $\Delta_m = 1 \pm a \sin(q\Delta_m)$. For a given value of Δ_m , there are an infinite number of contours in the $a - q$ plane which have identical shapes but are displaced from one another according to $q_n(a) = q_0(a) + n(\pi/\Delta_m)$, where n is an integer. Figure 2 shows a set of contours corresponding to q_0 , which is the relevant branch if the wisps have simple brightness contours with a single maximum at $y = 0$. For ripples of fixed amplitude a , the maximum possible enhancement, $\Delta = a + 1$, occurs for $\cos(qa + q) = 0$.

From the definition of q , we see that the maximum value of q for fixed x occurs at $y = 0$. Thus, if the wisps are to be brightest on the leading and trailing sides of the wave-front (i.e., at $y = 0$), we must have $\partial\Delta_m/\partial q|_a > 0$. For the q_0 branch, this corresponds to the condition $kH \cot\theta < \pi/(2a+2)$. Figure 3 shows a representative surface brightness plot for this case.

Narrower structures with higher brightness contrasts are possible if the emissivity of the equatorial zone is non-uniform. In particular, we might expect the slab to be edge-brightened, since the magnetic field strength will decline towards the center of the slab (since it reverses sign in this region), and the acceleration of relativistic electrons might also be greatest in the regions of strong shear and large field gradients. If the emissivity is confined to a fraction ξ of the slab’s thickness, then the maximum surface brightness contrasts will be enhanced by an additional factor of $\sim \xi^{-1}$. We would also expect to see a doubling of the wisp structures, for which there may be evidence in the WFPC2 image presented by Hester et al. (1995; Fig. 8).

4. DISCUSSION

I have proposed that the moving wisps near the center of the Crab Nebula can be interpreted as long-wavelength Kelvin-Helmholtz instabilities in the equatorial zone of the shocked pulsar wind. This interpretation explains why the wisp pattern persistently moves outward from the pulsar,

as revealed in recent observations (e.g., Tanvir et al. 1997), instead of remaining stationary or oscillating in position. It also explains the apparent confinement of the wisps to a plane oriented perpendicular to the inferred pulsar rotation axis. The observed pattern speeds of $\lesssim c/3$ are consistent with equatorial outflow velocities of $\gtrsim 0.6c$, shearing against a high-latitude flow with speeds of much less than $c/3$. If the speed of the high-latitude flow is taken into account, constraints on the equatorial flow speed are relaxed somewhat.

The wisps’ appearance as narrow, high-intensity arcs of emission need not imply that they are dissipative structures. They could simply be geometric artifacts resulting from the projection of our line of sight through the rippled, radiating slab. Such an interpretation is workable provided that the dominant K-H modes have sufficiently long wavelengths ($k_R H \lesssim 0.05$) and large amplitudes. At such large amplitudes, nonlinear effects (secondary instabilities, etc.) may be important, and the actual shapes of the ripples are likely to be far from the simple sine wave I assumed in § 3 for illustrative purposes. Dissipative processes (e.g., second-order Fermi acceleration, reconnection) could be associated with the complex nonlinear flow so one cannot rule out the possibility that localized dissipation contributes to the appearance of the wisps. To reconcile the observed spacing of the wisps with the geometric model for their appearance would require the sheet to be thin indeed, $H/r \lesssim 0.01$, where r is the radial distance of the wisps from the pulsar. Note that our model for the Kelvin-Helmholtz instability is simplified by assuming a “top-hat” velocity profile rather than a smooth gradient, but this detail should not be important for such small values of kH .

A more substantial worry is the stringent requirement on the slab’s emissivity compared to that of its surroundings. To avoid the wisps’ being drowned out by a bright background, the equatorial zone’s intrinsic emissivity would have to be many times larger than that of the high-latitude regions, since the latter occupy so much more volume. At

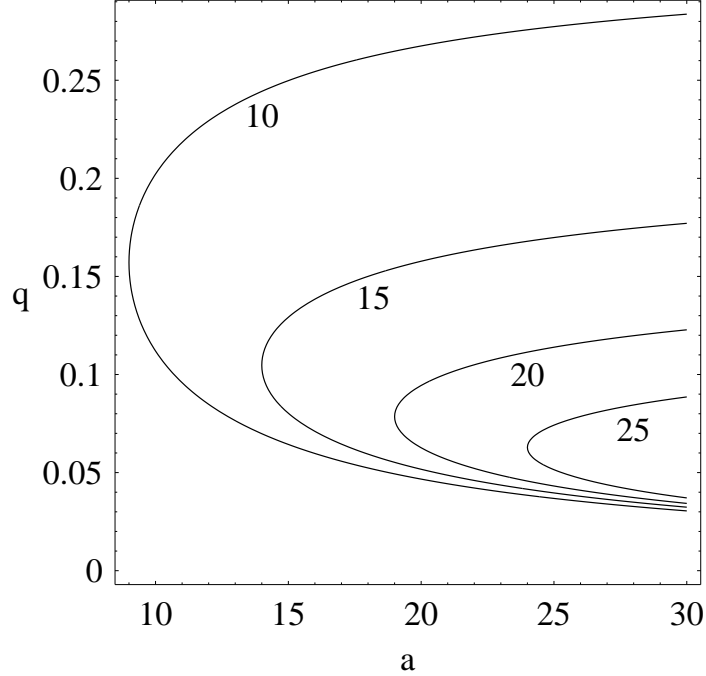


FIG. 2.— Contours of maximum brightness enhancement due to viewing geometry through a uniformly emitting rippled slab, in the $a - q$ plane. a is the amplitude of the ripples in units of slab thickness H and q is the product of scaled wavenumber kH with geometric factors. Contours are labeled with the value of the brightness enhancement factor, Δ_m .

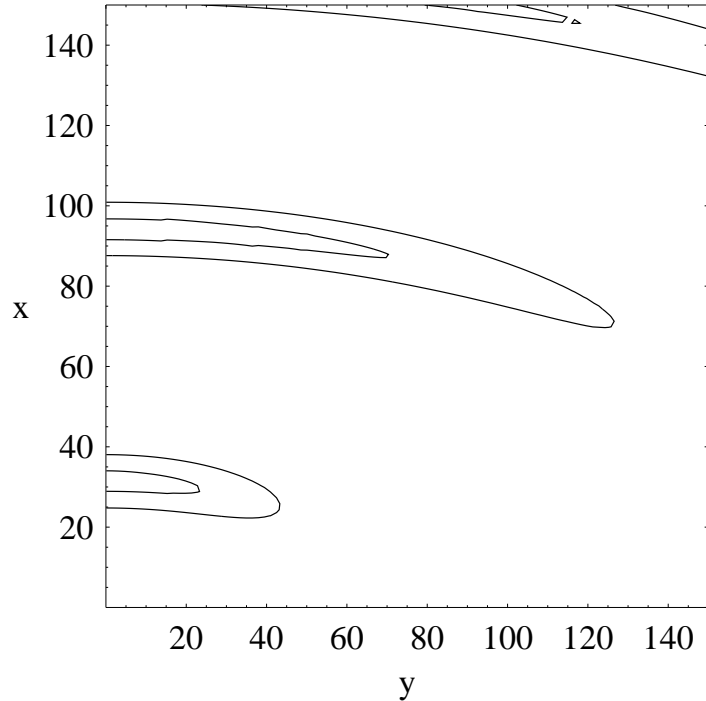


FIG. 3.— Surface brightness map of a rippled slab with $kH = 0.05$, $a = 15$, and $\theta = 30^\circ$. Displacements on the sky are scaled in units of kH and only one quadrant is shown. The nested contours correspond to brightness enhancement factors of 10 and 15 relative to the background; contrast can be increased by decreasing kH and increasing a . Compare the morphology to Figures 1 and 2 in Tanvir et al. (1997) and Figure 8 in Hester et al. (1995).

present I have no explanation for why this should be the case, although one might suspect that particle acceleration is especially efficient near the neutral sheet, where the magnetic fields are highly dynamical and reconnection may be occurring.

I have tentatively identified the equatorial zone with the "neutral sheet" across which the direction of the toroidal magnetic field reverses. The physical thickness of the shear layer (H) is presumably determined by physical processes occurring in the field-reversal region. Why should there be shear between the equatorial zone and the high-latitude regions of the wind, especially downstream of the main wind shock where one might expect both regions to be decelerated to $c/3$? One possibility is that the equatorial zone has a higher ram pressure upstream of the shock, because of uncertain physical processes near the base of the pulsar wind. (Note that the ram pressure has components due to both the particle flux and the Poynting flux.) When the high-latitude wind shocks it is slowed down to $\sim c/3$ and subsequently decelerates further, but the plasma in the equatorial zone punches through the shock radius with little change in velocity. The equatorial zone then comes into pressure equilibrium with the high-latitude shocked wind through a system of oblique shocks, which slows it somewhat but still can leave substantial shear.

It is also possible for the equatorial wind zone to accelerate relative to the high-latitude wind, even if both regions initially co-move at $\sim c/3$ after passing through a strong shock upstream of the wisps. The reason is that the high-latitude wind is more highly magnetized than the plasma in the equatorial zone where, effectively, the magnetic field vanishes. If the high-latitude wind maintains a well-organized toroidal field downstream of the shock, then the *total* pressure (gas + magnetic) in the decelerating high-latitude wind will actually *decrease* with radius, due to the effects of magnetic tension (Begelman & Li 1992). The equatorial zone will try to maintain pressure balance with the high-latitude wind but, because its magnetization is much smaller, it will respond to the pressure gradient by accelerating. The bulk Lorentz factor in adiabatic flow of an unmagnetized relativistic fluid varies as $p_{\text{tot}}^{-1/4}$. Thus, in order for the equatorial zone to accelerate from $u_0 = 1/3$ to $u = 0.5, 0.6$, or 0.7 , the pressure would have to drop to $0.71, 0.52$, or 0.33 of its value immediately outside the shock. Such pressure drops are possible provided that the magnetic pressure in the high-latitude wind is not much smaller than the gas pressure (Begelman & Li 1992).

A near-equipartition magnetic field in the wisp region is seriously at odds with widely accepted theoretical models of the Crab Nebula (Rees & Gunn 1974; Kennel & Coroniti 1984; Emmering & Chevalier 1987), which imply that the magnetic pressure in the wisp region is only a couple of percent of the gas pressure. (This is consistent with a ratio of Poynting flux to kinetic energy flux in the pre-shock wind of $\lesssim 0.003$.) However, this inference depends critically on the assumption that an axisymmetric toroidal field structure is maintained throughout the nebula. Begelman (1998) has pointed out that such a field geometry is highly unstable, and that the rearrangement of the field will se-

riously weaken any theoretical upper limits on the wind's magnetization. One cannot rule out the possibility that the shocked wind is sufficiently magnetized to sustain a modest pressure drop, before reaching radii beyond which instabilities wash out further pressure gradients.

Because of the many uncertainties regarding the structure of the Crab pulsar wind and its nebular environment, it may prove difficult to devise definitive observational tests of the model presented in this paper. However, if the model is correct qualitatively, we expect the following observational trends:

1. An inverse relationship between wisp spacing and pattern speed. If the wisps represent the nonlinear development of the Kelvin-Helmholtz instability, we should not be surprised to find fluctuations in the wisp spacing and pattern speed, even if the wind and main shock system are relatively steady. Since the wavelength and phase velocity are inversely correlated for long-wavelength K-H modes (with $v_p \propto \lambda^{-1/2}$ asymptotically), there should be a qualitatively similar relationship between wisp spacing and pattern speed. This is probably the most distinctive prediction of this model, compared to others. (For example, the pattern speed of magnetosonic waves should be independent of wavelength.)
2. Possible lack of evidence for localized dissipation in the wisps. If the wisps were dissipative structures, one might expect to see evidence of fresh particle acceleration (e.g., flattening of the synchrotron spectrum) associated with the brightest features. If the wisps are instead artifacts of the viewing geometry, then the spectrum should not be correlated with surface brightness. (Note that this test may be complicated by systematic variations of the emitted spectrum with height within the equatorial layer.) This characteristic is shared by other models in which the wisps arise from adiabatic compression of relativistic particles, e.g., in the model of Gallant & Arons (1994) and the synchro-thermal instability of Hester et al. (1995).
3. Doppler asymmetry of the approaching and receding wisps. A careful analysis of the brightness asymmetry should be consistent with bulk flow velocities somewhat *larger* than the pattern speeds. It will be important to take into account light travel time effects as well as aberration of the observed ripple pattern. This should be a general characteristic of any model in which the outward pattern speed is slower than the underlying fluid velocity, i.e., it should apply in propagating wave models provided that the waves propagate *inward* relative to the fluid.

I am grateful to Martin Rees and Ellen Zweibel for helpful discussions, and to the anonymous referee for constructive criticism. This work was supported in part by National Science Foundation grant AST-9529175.

REFERENCES

Barnes, A., & Scargle, J. D. 1973, *ApJ*, 184, 251
 Begelman, M. C. 1998, *ApJ*, 493, 291
 Begelman, M. C., & Li, Z.-Y. 1992, *ApJ*, 397, 187
 Chedia, O., Lominadze, J., Machabeli, G., Mchedlishvili, G., & Shapakidze, D. 1997, *ApJ*, 479, 313
 Emmering, R. T., & Chevalier, R. A. 1987, *ApJ*, 321, 334
 Ferrari, A., Massaglia, S., & Trussoni, E. 1982, *MNRAS*, 198, 1065
 Gallant, Y. A., & Arons, J. 1994, *ApJ*, 435, 230
 Gill, A. E. 1965, *Phys. Fluids*, 8, 1428
 Hardee, P. E., Cooper, M. A., Norman, M. L., & Stone, J. M. 1992, *ApJ*, 399, 478
 Hardee, P. E., & Norman, M. L. 1988, *ApJ*, 334, 70
 Heinz, S., & Begelman, M. C. 1997, *ApJ*, 490, 653
 Hester, J. J., et al. 1995, *ApJ*, 448, 240
 Kennel, C. F., & Coroniti, F. V. 1984, *ApJ*, 283, 694
 Kundt, W., & Krotscheck, E. 1980, *A&A*, 83, 1
 Lampland, C. O. 1921, *PASP*, 33, 79
 Lou, Y.-Q. 1996, *MNRAS*, 279, 129
 Lou, Y.-Q. 1998, *MNRAS*, 294, 443
 Norman, M. L., & Hardee, P. E. 1988, *ApJ*, 334, 80
 Oort, J. H., & Walraven, T. 1956, *BAN*, 12, 285
 Payne, D. G., & Cohn, H. 1985, *ApJ*, 291, 655
 Rees, M. J., & Gunn, J. E. 1974, *MNRAS*, 167, 1
 Scargle, J. D. 1969, *ApJ*, 156, 401
 Tanvir, N. R., Thomson, R. C., & Tsikarishvili, E. G. 1997, *NewA*, 1, 311
 Trimble, V. 1982, *Rev. Mod. Phys.*, 54, 1183
 Woltjer, L. 1958, *Bull. Astr. Inst. Netherlands*, 14, 39